One of us, A. W. C., would like to thank the Science Research Council for a research studentship during the tenure of which this work was carried out.

I. P. WILLIAMS
A. W. CREMIN

Department of Mathematics,
University of Reading.

Received October 27, 1967.

[1] Walker, M. F., *Ap. J. Suppl.*, **2**, 365 (1956).
[2] Walker, M. F., *Ap. J.*, **125**, 636 (1957).
[3] Walker, M. F., *Ap. J.*, **130**, 57 (1959).
[4] Whiteoak, J. B., *Mon. Not. Roy. Astro. Soc.*, **123**, 245 (1961).
[5] Henyey, L. G., LeLevier, R., and Levée, R. D., *Pub. Astro. Soc. Pacific*, **67**, 154 (1955).
[6] Huang, S. S., *Ap. J.*, **134**, 12 (1961).
[7] McCrea, W. H., and Williams, I. P., *The Observatory*, **82**, 245 (1962).
[8] Williams, I. P., *The Observatory*, **87**, 26 (1967).
[9] Hayashi, C., *Pub. Astro. Soc. Japan*, **13**, 450 (1961).
[10] Faulkner, J., Griffiths, K., and Hoyle, F., *Mon. Not. Roy. Astro. Soc.*, **126**, 1 (1963).
[11] Ezer, D., and Cameron, A. G. W., *Icarus*, **1**, 422 (1964).

PLANETARY SCIENCE

Upper Atmosphere Density in 1966–67: the Dominance of a Semi-annual Variation at Heights near 200 km

ANALYSES of the changes in satellite orbits have established that the principal variations in upper atmosphere density at heights between 180 km and 1,000 km are attributable to solar activity and differences between day and night. A further effect, usually smaller, is the semi-annual variation, with maximum densities in April and October and minima in January and July. These results are embodied in the *Cospar International Reference Atmosphere*[1] and other models of the upper atmosphere.

Solar activity has been greater and more variable during 1967 than during 1966, and might have been expected to exercise a dominating influence over upper-atmosphere density during 1967. This expectation has not been fulfilled, however, particularly at heights near 200 km. A recent analysis of the orbit of the satellite Secor 6 (1966–51*B*) has yielded 154 values of air density at a height of 191 km at dates between June 14, 1966, and July 5, 1967. These results, which will be reported in detail elsewhere, show that solar activity, as represented by the radiation energy at a wavelength of 10·7 cm, did not exercise appreciable influence over the air density. Nearly all the nineteen large geomagnetic disturbances occurring during the life of the satellite were accompanied by sharp increases in air density for a few days; but, when these disturbed days are eliminated, the remaining variations in density are apparently quite unrelated to the wide variations in the 10·7 cm radiation energy, which shows a strong 27-day recurrence over much of the satellite's life in orbit.

The values of air density obtained from the orbit of Secor 6 at a height of 191 km are shown in Fig. 1, after removing geomagnetically disturbed days and making small corrections for the long-term increase in solar activity and for day-to-night variations in density. (Values between August 23 and September 17, 1966, are regarded as doubtful, because of lack of data and also because several points at times of geomagnetic disturbance had to be removed.) The chief feature of Fig. 1 is a semi-annual variation, with maxima of about $5{\cdot}0 \times 10^{-10}$ kg/m^3 in October 1966 and April 1967, and minima (excluding the doubtful September values) in July 1966 and January 1967 of about 3·7 and $3{\cdot}2 \times 10^{-10}$ kg/m^3, respectively. These values are averages over about 30 days, rather than extreme maxima or minima. This semi-annual variation, with the maximum density exceeding the minimum by a factor of 1·45, has been in many respects the most important variation in upper-atmosphere density during 1967 at heights near 200 km, and has significantly affected the accuracy of satellite lifetime estimates.

The semi-annual variation in air density, found from the orbit of Echo 2 by Cook and Scott[2] at a height of 1,130 km at dates up to January 1967, is almost identical in form to the left-hand half of Fig. 1, although the numerical values of density are lower by a factor of more than 10^5 at 1,130 km height. This confirms that the density variations apparent in Fig. 1 are dependent on date.

The apparent failure of solar activity to influence upper-atmosphere density at heights near 200 km, except through the short-lived solar outbursts which give rise to geomagnetic storms, suggests that the radiation responsible for controlling upper-atmosphere density during the declining years of the last sunspot cycle may not be as strong during the rising part of the current cycle.

D. G. KING-HELE

Royal Aircraft Establishment,
Farnborough, Hampshire.

Received November 3, 1967.

[1] *Cospar International Reference Atmosphere 1965* (Amsterdam, North Holland, 1965).
[2] Cook, G. E., and Scott, D. W., *Planet Space Sci.* (in the press).

Differences of Composition among Australian Iron Meteorites

THE discovery[1] of iron meteorite fragments with the structure of medium octahedrites in the neighbourhood of the Wolf Creek meteorite crater compounded a curiosity. The Boxhole and Henbury craters were already known to be associated with meteoritic debris which has the structure of medium octahedrites and although such structures are relatively common among iron meteorites—Hey's[2] catalogue shows them to represent 36 per cent of all classified irons—coincidence of structures has caused speculation that two or more of these cratering events were produced by fragments of the same meteoroid.

The Boxhole and Henbury craters lie about 300 km apart along the N.E.–S.W. line in central Australia (Northern Territory). Wolf Creek is located in western Australia about 850 km N.W. of this area, and thus the three objects do not lie along an arc of the Earth's surface. Although such distances are small by Australian standards, they are much greater than the linear dimensions of any known meteoritic strewn field, as recently discussed by

(*Continued on page 905*)

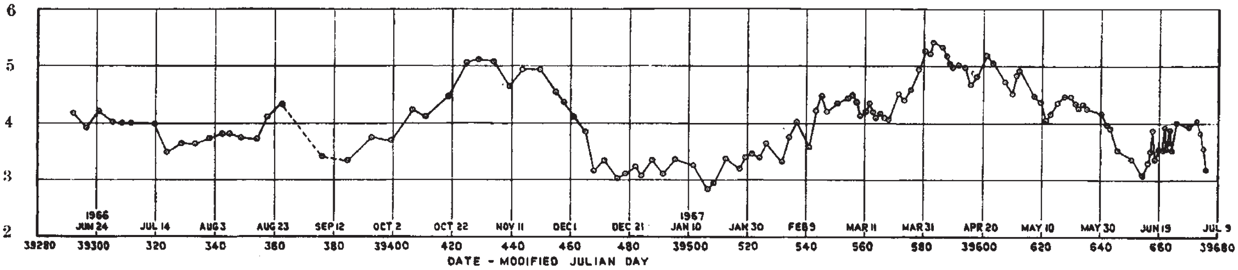

Fig. 1. Values of density, ϱ_F at a height of 191 km, averaged between day and night, with geomagnetic storms excluded.

(*Continued from page 880*)

Table 1. CONCENTRATIONS OF NICKEL, GALLIUM, GERMANIUM AND IRIDIUM

Meteorite	Nickel (per cent)	Gallium (p.p.m.)	Germanium (p.p.m.)	Iridium (p.p.m.)
Boxhole	7·64	18·1	37·2	9·1
Henbury	7·44	17·4	34·2	15·0
Wolf Creek	9·23	18·4	37·3	0·040

Wasson and Goldstein[3], so it would have been especially interesting if a relationship were found between two or more of these objects.

Recent work has shown that detailed studies of the chemical composition of iron meteorites can be used to classify these objects into chemical groups, and in addition to define the relationship of the meteorite within a particular group[3–5]. Studies of the Chilean hexahedrites[3] and of the Arizona octahedrites[5] have provided strong evidence that fragments of the same fall tend to be extremely similar in composition. Thus a study of the three Australian irons offered the possibility of testing for compositional indications of a relationship among them.

We have found that most medium octahedrites fall into one or the other of two closely related groups designated IIIA and IIIB. Group IIIA includes irons with 7·4–8·7 per cent nickel, 18–22 p.p.m. gallium, 33–46 p.p.m. germanium, 0·4–17 p.p.m. iridium and structures intermediate between medium and coarse octahedrites. Group IIIB includes objects with 9·2–10·7 per cent nickel, 16–20 p.p.m. gallium, 28–38 p.p.m. germanium, 0·01–0·1 p.p.m. iridium and structures ranging from medium to fine octahedrites. Gallium and germanium are positively correlated with nickel in group IIIA and negatively correlated with nickel in group IIIB. The correlation of iridium with nickel is negative in group IIIA and not yet defined in group IIIB. Nickel has been determined by atomic absorption, and gallium, germanium and iridium by neutron activation.

Table 1 shows the results of duplicate determinations of the four elements in a specimen from Wolf Creek, provided by S. R. Taylor, and in specimens from Boxhole and Henbury, from the Leonard Collection of meteorites at this university. Nickel, gallium and germanium results for the latter two objects are essentially the same as those reported earlier[4]. Each iron is observed to be unique in composition. There is some overlap in the gallium and germanium contents, but the differences in nickel and iridium concentration are substantially greater than experimental errors. 95 per cent confidence limits are about 1·5 per cent of the reported nickel concentrations, about 10 per cent of the higher iridium values. The Wolf Creek iridium result may be in error by as much as 30 per cent. Boxhole and Henbury are found to be typical low nickel members of group IIIA, whereas Wolf Creek is a typical low nickel member of group IIIB.

This evidence clearly indicates that each of these craters was formed by a unique event. A simple calculation shows that the likelihood of three such events occurring in succession is not unreasonably small. If the probability of the Earth capturing crater-forming irons of a given structural class is given by the fall statistics cited here for small objects, the probability of three successive cratering events by medium octahedrites is $(0·36)^3$, or a respectable 0·05. The probability is even higher if it is considered that the first event was class-establishing and should be considered separately.

JOHN T. WASSON

Department of Chemistry and
Institute of Geophysics and Planetary Physics,
University of California, Los Angeles.

Received October 16, 1967.

1 Taylor, S. R., *Nature*, **208**, 944 (1965).
2 Hey, M. H., in *Catalogue of Meteorites* (British Museum, London, 1966).
3 Wasson, J. T., and Goldstein, J. I., *Geochim. Cosmochim. Acta*, **32** (in the press).
4 Wasson, J. T., and Kimberlin, J., *Geochim. Cosmochim. Acta*, **31**, 2065 (1967).
5 Wasson, J. T., *J. Geophys. Res.* (in the press).

Diffracted S

Gutenberg and Richter[1] commented in 1935 that diffracted *S* (the *S* wave diffracted around the Earth's core) was recorded more frequently than diffracted *P*, but they provided no observational data. To our knowledge, the only reference to observations of *S* beyond the shadow zone since that time was made by Lehmann[2], who expressed doubt (on the score of amplitude) whether this or the corresponding *P* phase were really diffracted waves. Again, no details of arrival times were given. The scant attention paid to diffracted *S* may be attributed to the fact that it is not listed in the standard travel time tables and consequently is not reported in station bulletins. On the other hand, observations of diffracted *P* are common, because it appears on seismograms as the first arrival at distances beyond about 100°.

Duwalo and Jacobs[3], in a theoretical study of diffraction around a liquid core, have shown that *SH* waves can be diffracted around the core boundary. At the same time, they pointed out that a diffracted *SV* wave is not possible, because no shadow zone exists between *S* and *SKS*. This provides a criterion for the identification of diffracted *S*, because core phases such as *SKS* and *SKKS* must emerge as *SV* waves[4].

On a number of occasions we have observed, on Canberra records, a phase which satisfies this criterion from earthquakes at distances between 99° and 130°. The phase is detected on long period Press-Ewing horizontal seismometers ($T_s = 30$ sec, $T_g = 100$ sec) as a single-cycle wave with a period of about 20 sec. It occurs about midway between *SKKS* and *PS*, where no other arrival of *S* type is expected, and can be readily identified in routine analysis of the seismograms.

Table 1 gives details of the earthquakes and the observed travel times, based on information from USCGS *PDE* cards. The first two events, both from Pakistan, illustrate a method of determining the distance at which *S* grazes the core–mantle boundary. The particle motion of *S* from the event at 98·8° distance is unpolarized, while for the other, at 99·6°, it is strongly polarized in the *SH* direction. This implies that the change from *S* to diffracted *S* takes place between these two distances, although further data are needed for verification of the result. No comparable method exists for determining the change from *P* to diffracted *P*.

Records of three events included in the table are shown in Fig. 1. The *SH* nature of the phase can be seen most clearly in the arrivals from Mexico and Panama. Waves from these earthquakes approach Canberra from azimuths which are almost due east. In both cases, the diffracted *S* arrival appears on the N.–S. seismogram, while the core phases are present on the E.–W. records. Lehmann[2] likewise noted that two Chilean earthquakes at distances of 106° and 116° and azimuths W.S.W. from Copenhagen gave an *S* phase visible only on the N.–S. record at Copenhagen. A striking feature of the Panama records is the large amplitude of diffracted *S* relative to the other phases. We surmise that the fault motion was at right

Table 1

Date	Origin time (G.M.T.)	Location	Epi-central distance (deg)	Depth (km)	Magni-tude	*S* travel time min sec
Feb. 7, 66	04 26 14	Pakistan	98·8	33	6·0	25 10
Aug. 1, 66	21 03 00	Pakistan	99·6	33	6·2	25 18
Dec. 22, 65	19 41 23	Kodiak Is.	105·1	50	6·5	26 03
Dec. 6, 65	11 34 54	Mexico	111·8	37	6·0	27 06
Mar. 20, 66	01 42 50	Uganda	113·6	36	6·1	27 36
Dec. 9, 65	06 07 49	Mexico	116·8	57	6·0	27 39
Feb. 15, 67	16 11 12	Peru–Brazil	121·8	597	6·2	26 34
Sept. 17, 65	13 13 56	Ecuador	123·2	190	6·0	28 14
Sept. 9, 65	10 02 25	Central America	123·3	27	5·9	28 59
Aug. 19, 66	12 22 10	Turkey	123·5	26	6·1	28 40
Dec. 15, 65	23 05 21	S. of Panama	125·6	15	6·0	29 19
Feb. 9, 67	15 24 47	Colombia	128·1	58	6·3	29 07